Final Report

Remediation of Explosives Contaminated Groundwater With Zero-Valent Iron

SERDP Project ER-1232

October 2011

Paul Tratnyek
Richard Johnson
Oregon Health & Science University

This document has been cleared for public release

SERDP
DOD ▪ EPA ▪ DOE

Abstract

A series of laboratory and field studies was performed to evaluate the in situ degradation of TNT and RDX using permeable reactive barriers (PRBs) made with zero-valent iron (ZVI). The disappearance of both TNT and RDX were shown to be rapid in the laboratory and ex situ field columns. Batch experiments performed with ^{14}C-labelled TNT have showed that the products of reaction with iron metal are partly sequestered on the metal (oxide) particle surfaces. Most of the bound residue could not be solubilized using a range of extraction procedures. However, batch studies over a range of experimental conditions show considerable variability in the degradation products, while the primary TNT degradation product in column studies is TAT.

Ex situ column experiments at the Umatilla Chemical Weapons Depot were used to examine the viability of the ZVI under field conditions. This site is challenging because the dissolved oxygen concentration is high. A series of column experiments were conducted at the site: including columns with 10%, 20%, 30%, and 100% iron by volume is silica sand. In all of these cases, oxygen is rapidly scrubbed from the water by the iron. For the low iron cases, oxygen and RDX breakthrough occurred after several thousand of pore volumes. The columns with higher iron content (30%, 100%) plugged after time. In at least some cases this was due to particulates coming from the column.

Table of Contents

List of Figures

List of Tables

List of Acronyms

[Fe(0)]	Concentration of iron
[S_a]	Concentration of reactive surface sites
a_s	Specific surface area
DNT	Dinitrotoluene
DoD	Department of Defense
FePRB	Iron permeable reactive barrier
HMX	Octahydro-1,3,5,7-tetranitro-1,3,5,7-tetrazocine
K	Permeability
k_0	Zero-order rate constant
k_1	First-order rate constant
$K_{1/2}$	Half-saturation constant
k_M	mass-normalized reaction rate
k_{obs}	observed reaction rate
k_{obs}	Observed, pseudo-first order rate contant
k_{SA}	surface-area-normalized reaction rate
k_{SA}	Surface-normalized rate constant
PRB	Permeable reactive barrier
RDX	1,3,5-Trinitroperhydro-1,3,5-triazine
TAT	Triaminotoluene
TNT	Trinitrotoluene
V_m	Maximum reaction rate
ZVI	Zero-valent iron
Γ	Concentration of surface sites
λ	Fraction
ρ□	Mass concentration of iron

Background

Statement of the Problem

Most explosives that occur as groundwater pollutants at DoD sites are nitro aromatic compounds (TNT, trinitrobenzene, and various di- and mono-nitrotoluenes) or nitramines (RDX, HMX, and Tetryl). Under favorable conditions, most of these compounds react rapidly with zero-valent iron, which suggests that permeable reactive barriers containing zero-valent iron (FePRBs) might be useful for remediation of groundwater contaminated with explosives.

However, all of the early work on explosives reduction by Fe(0) was done as batch experiments with nitro aromatic compounds, and this system produces solution-phase aromatic amines as the major products (e.g., Arienzo, 2000; Hundal et al., 1997; Oh et al., 2002a). Since these products are still substances of regulatory concern, full-scale implementation of FePRBs to treat explosives contaminated groundwater was delayed while complementary methods for treatment of the amines were investigated.

In our work funded under SERDP SEED project (CU-1176), however, we found that column model systems—which are more representative of the conditions used in full-scale remediation operations—remove very large quantities of TNT without allowing breakthrough of any degradation products that are identifiable by HPLC. The unexpected absence of TAT or other degradation products in the column effluent (in contrast to what we and others have observed in batch experiments) was hypothesized as being due to greater sequestration on Fe(0) under conditions representative of those encountered in field applications. This sequestration may be due to adsorption, coprecipitation with iron oxides, and/or polymerization of reduction products, and is likely to be largely irreversible. Analogous processes were expected for RDX and other nitramine explosives.

Furthermore, we observed considerable variability in the proportion of TNT reduction products that become bound residues. Soluble reduction products are favored when TNT is exposed to larger concentrations of iron and to iron that has been allowed to equilibrate with the aqueous medium for longer periods of time. These factors allow laboratory batch experiments to favor sequestered products, while experiments performed in columns produce mainly soluble reduction products. Understanding precisely what controls the branching among the monomer and the polymer formation pathways is essential, so that information can be used to design operating conditions that achieve the

most desirable end-point in field-scale implementation of Fe(0) to remediation explosives contaminated groundwater.

Project Goals and Objectives

The overall goal of this project was to determine how operating conditions influence the distribution of products from the reduction of TNT, with the ultimate goal of defining optimal operating conditions for reaching remediation goals. The original project was organization into objectives and tasks is shown in Table 1.

Table 1. Summary of the Original Technical Objectives and Tasks

Objective 1. Obtain a detailed characterization of contaminant removal using *bench-scale reactors.*
• Task 1. Complete a comprehensive *mass balance* of the products (both dissolved and sequestered) for TNT and RDX reacting with Fe(0).
• Task 2. Resolve the *kinetics* of reaction from adsorption for TNT and RDX using steady-state and pulse elution experiments with small columns of Fe(0).
• Task 3. Load columns with TNT and systematically vary operating parameters to analyze potential desorption of TNT or products.
Objective 2— Evaluate options for design and implementation of *pilot-scale treatment zones* of Fe(0).
• Task 4. Perform pilot-scale test with above columns of granular Fe(0) using the pump and treat system at the *Umatilla Weapons Depot*.
• Task 5. Develop reactive transport *model* (using process and parameter information obtained from Tasks 1-4) for use in designing full-scale, in situ FePRBs for explosives.

The work performed addressed all of the objectives and tasks listed above. The work includes experimental results from laboratory batch, laboratory column, and field pilot experiments. Modeling results were also used to provide more precise interpretation of individual experiments and to put individual experimental results into the broader context provided by a comprehensive deterministic model of contaminant interactions with Fe(0). In accord with the project timeline, shown in Table 2, the first part of this report summarizes our results on the project tasks for bench-scale work. The second part of this report summarizes the results from the pilot-scale work involving ex situ columns at the Umatilla Weapons Depot.

Table 2. Timeline of tasks from the project proposal. Solid bars represent primary activities, and striped bars represent secondary (preliminary or follow up)

	Project Year 1				Project Year II			
Group/Tasks	1/4	2/4	3/4	4/4	1/4	2/4	3/4	4/4
Objective 1, Task 1—Mass Balance								
Objective 1, Task 2—Kinetics								
Objective 2, Task 3—Desorption								
Objective 2, Task 4—Umatilla								
Objective 2, Task 5—Modeling								

Results

For the purposes of this report, we have organized our results in a manner that roughly follows the tasks and timeline of the original project proposal. However, we have included section breaks and headings to reflect how the project results have been grouped into manuscripts for publication. In each case, the publication is identified in a footnote to the section heading.

Disappearance Kinetics (Task 2)[1,2,3,4]

We found that the kinetics of TNT disappearance are more complex than has generally been observed in batch experiments with other contaminants. Rather than fitting the disappearance data to a pseudo first-order kinetic model, as is usually done (Johnson et al., 1996), our results with TNT suggest that a mixed-order kinetic model is often more appropriate.

For the purposes of this study, it is convenient to express our mixed-order kinetic model for site saturation limited kinetics in terms that are commonly used for enzyme catalyzed reactions, as we have in several publications (Agrawal et al., 2002; Johnson et al., 1998; Johnson et al., 1996; Nam and Tratnyek, 2000). This model can be written:

$$-\frac{dC}{dt} = \frac{V_m C}{K_{1/2} + C} \qquad [1]$$

where V_m is the maximum reaction rate and $K_{1/2}$ is the concentration of contaminant, C, where $-dC/dt = V_m/2$. Note that V_m is equivalent to the rate constant for the zero-order portion of the progress curve and that $V_m/K_{1/2}$ approximates the rate-constant for the first-order portion (represented by k_0 and k_1, respectively, in Wüst et al. (Wüst et al., 1999)).

To apply the model represented by equation 1, we used the bisection method (Press et al., 1988) to solve the integrated form of equation 1 for C as a function of V_m, $K_{1/2}$, C_0, and t, and this result was fit to experimental data by chi-square minimization. The details of this analysis are published in Tratnyek et al. (Tratnyek et al., 2002) and

---

[1] Tratnyek, P. G.; Miehr, R.; Bandstra, J. Z. (2002) Kinetics of reduction of TNT by iron metal; *Groundwater Quality 2001: Third International Conference on Groundwater Quality,* Sheffield, UK, IAHS Press, Vol. 275, pp. 427-433.

[2] Miehr, R.; Tratnyek, P. G.; Bandstra, J. Z.; Scherer, M. M.; Alowitz, M.; Bylaska, E. J. (2004) The diversity of contaminant reduction reactions by zero-valent iron: role of the reductate. *Environ. Sci. Technol.*, 38(1): 139-147.

[3] Bandstra, J. Z.; Tratnyek, P. G. (2003) Effects of surface heterogeniety on the kinetics of interfacial electron transfer; *225th National Meeting, 23-27 March 2002,* New Orleans, LA, American Chemical Society, Vol. 43, No. 1, 541-545.

[4] Bandstra, J. Z.; Tratnyek, P. G. Applicability of single-site rate equations for reactions on inhomogenous surfaces. *Indus. Eng. Chem. Res.* 2004, *43*, 1615-1622.

closely parallel the kinetic modeling described in Agrawal et al. (Agrawal et al., 2002) for reduction of 1,1,1-trichloroethane by Fe(0). Figure 1 shows experimental data for two types of Fe(0) fit with the mixed-order kinetic model.

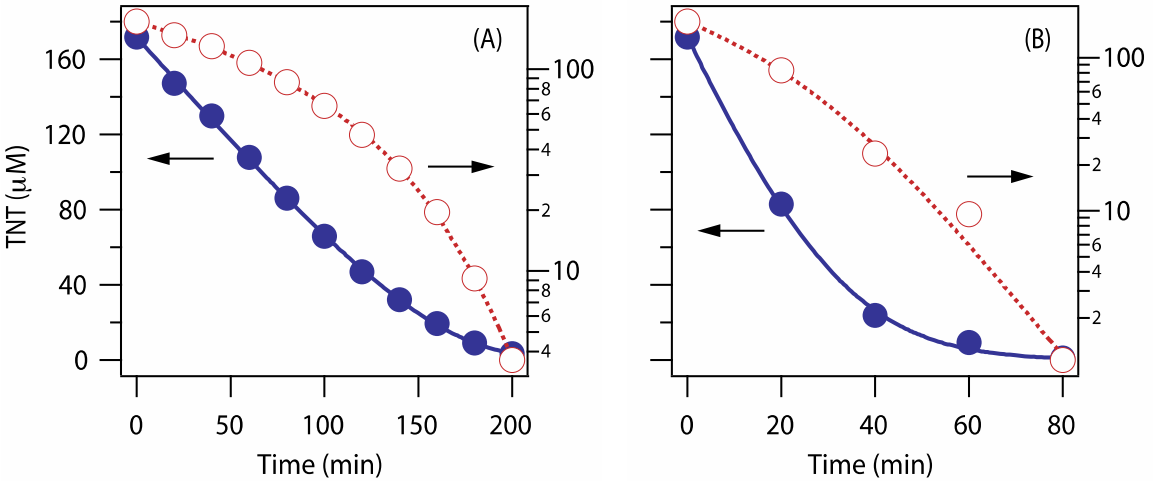

Figure 1. Kinetics of reduction of TNT in batch experiments with (A) Fluka iron and (B) Connelly iron. Results are plotted on linear (left) and log (right) axes. The curves reflect fits to the mixed-order kinetic model (i.e., equation 1). This figure is published in Tratnyek et al. (Tratnyek et al., 2002).

Although equation 1 provides an accurate description of TNT disappearance data for a wide range of conditions, the model is parameterized with two constants, V_m and $K_{1/2}$, rather than the single first-order rate constants that are frequently obtained from less-detailed studies. For comparison with previously reported kinetic data, we have calculated surface area normalized rate constants, k_{SA}, by equating $V_m/K_{1/2}$ with k_{obs} and dividing by the surface area concentration (m^2 of Fe(0) per L of solution).

Figure 2 shows these rate constants on a scale with other previously reported kinetic data for representative contaminants. Note that the values of k_{SA} for TNT are relatively small for Fe(0) types that contain a large amount of iron oxide (in green). This is because the iron oxide imparts a comparatively high specific surface area and low reactivity. Reagent-grade Fe(0) gives relatively high values of k_{SA} (other colors), consistent with the expectation that reagent-grade Fe(0) presents a relatively clean and smooth surface with high reactivity but lower specific surface area.

The kinetic model used in the results described above is based on Langmuir-Hinshelwood kinetics with one reactive surface site. However, some of our batch kinetic data shows features that cannot be described with this single-site model. Therefore, we explored more complex models with the hope of learning more about what controls the

rate of TNT disappearance in Fe(0)-water systems. We were particularly interested in obtaining a better understanding of how these processes scale from batch, to column, to field conditions.

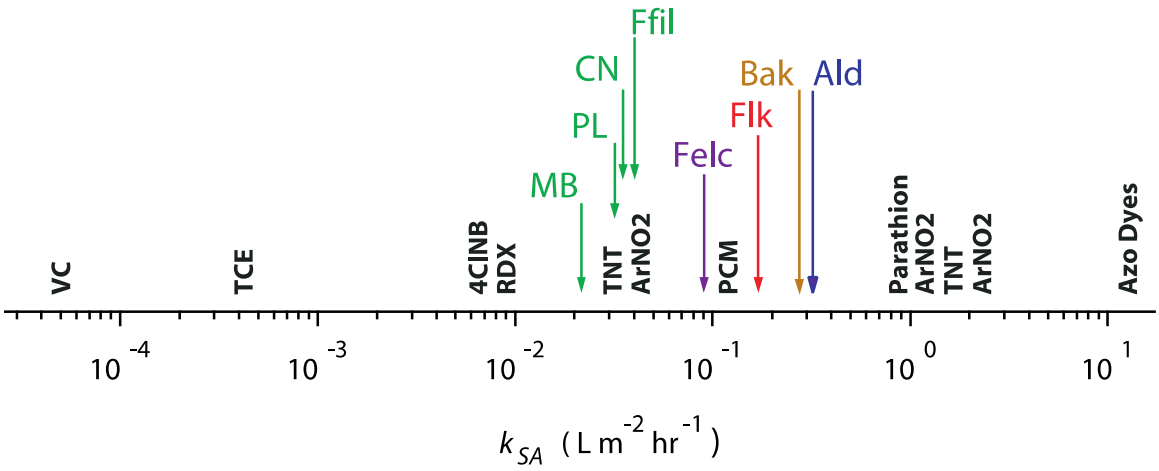

Figure 2. Comparison of k_{SA} from batch studies with TNT and eight types of iron (in color) vs. rate constants for other contaminants obtained from the literature. This figure is from Tratnyek et al. (Tratnyek et al., 2002), and it based on a figure in Scherer et al. (Scherer et al., 2001).

Figure 3 shows a comparison between one-site and two-site Langmuir-Hinshelwood kinetic model behavior, and a representative set of experimental data for the disappearance of TNT. It is apparent from these results that the two-site model provides a much more satisfactory description of the data. However, the lack of fit with a single-site model is not so severe that it would be apparent in studies where the data were less carefully scrutinized. More details on this model are given in (Bandstra and Tratnyek, 2003).

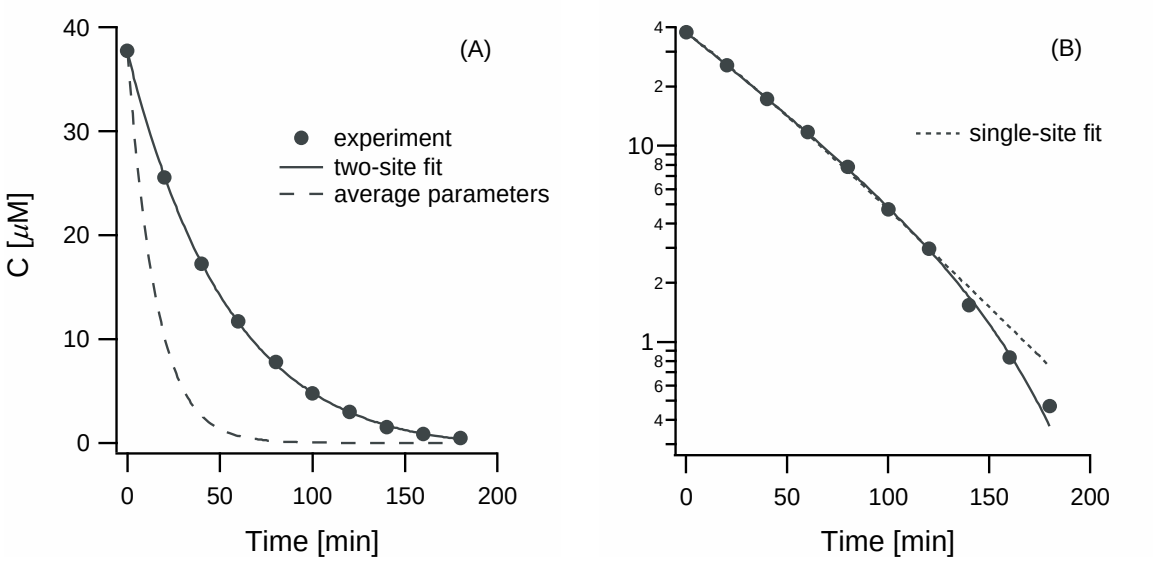

Figure 3. Modeling batch data for TNT reduction kinetics. (A) The two-site fit compared to the average parameter single-site model on a linear concentration scale. (B) The two-site fit compared to the single-site fit on a log transformed concentration scale. Data collected in batch experiments using 1.13 x 10^{-2} g mL^{-1} of Fisher Fe(0) filings (Tratnyek et al., 2002). This figure is adapted from (Bandstra and Tratnyek, 2003).

One of the implications of this analysis is that construction-grade Fe(0), which presumably offers a multi-site surface for reaction of TNT, might exhibit kinetics dominated by less reactive sites when the TNT concentration is high. If one fits a single-site kinetic model to these data, the resulting constants will under-predict reactivity of the Fe(0) at the lower TNT concentrations that are sometimes at issue in the field.

Products and Mass Balance (Task 1)[5,6]

We observed considerable variability in the detectable products of TNT reduction by Fe(0). Under typical batch experimental conditions, few reduction products were found in solution. However, increasing the concentration of Fe(0) used in batch

[5] Miehr, R.; Bandstra, J. Z.; Po, R.; Tratnyek, P. G. (2003) Remediation of 2,4,6-trinitrotoluene (TNT) by iron metal: Kinetic controls on product distributions in batch and column experiments; *225th National Meeting, 23-27 March 2002,* New Orleans, LA, American Chemical Society, Vol. 43, No. 1, 644-648.

[6] Bandstra, J. Z.; Miehr, R.; Johnson, R. L.; Tratnyek, P. G. (2005) Remediation of 2,4,6-trinitrotoluene (TNT) by iron metal: Kinetic controls on product distributions in batch. *Environ. Sci. Technol.*, 39(1): 230-238.

experiments (i.e., [Fe(0)]) resulted in the appearance of more products in solution and higher mass balances. Figure 4 illustrates this trend for batch experiments with 1, 2, and 6 grams of Fe(0). Additional data (not shown) confirms that this trend is systematic and reproducible.

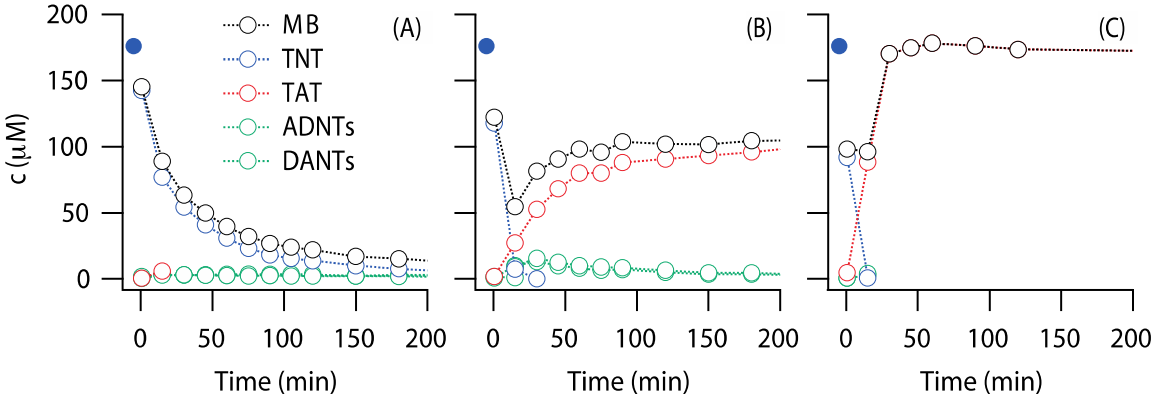

Figure 4. Results from batch experiments of TNT degradation using: (A) 1 g of Peerless iron, (B) 3 g, and (C) 6 g. In all cases, pre-exposure = 2 days, and $[TNT]_0$ = 176 μM (shown as solid blue points). Some additional details regarding these results are described in (Miehr et al., 2003b) and a complete analysis will be published as (Miehr et al., 2003a).

The trend of increased conversion of TNT to TAT with increased [Fe(0)] (shown in Figure 4) may indicate that reaction rates involving reduction of TNT and formation of TAT are limited by the transport of "electrons" from the underlying Fe(0) to the water/oxide interface. This type of phenomena has been anticipated (Scherer et al., 1998), but not investigated in any detail. We have modeled this process and the results are shown in Figure 5.

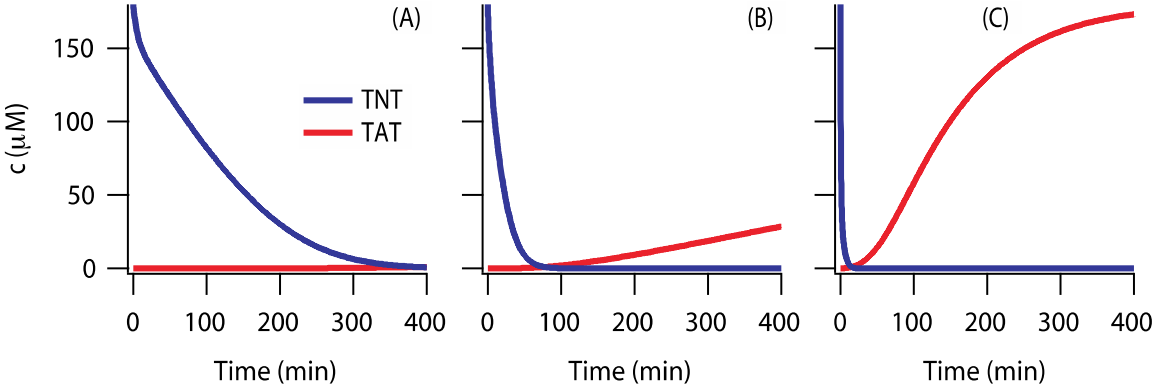

Figure 5. Simulated transformation of TNT to TAT showing the effect of reducing-site regeneration: (A) 1 g of Fe(0), (B) 3 g, and (C) 6 g. Relative values of rate constants

were constrained with a structure-activity relationship. Assuming $[\text{reducing sites}]_0$ = 5 per nm^2 and a regeneration rate that is proportional to the degree of surface site depletion.

For low [Fe(0)], the model shows that the initial supply of reducing sites at the interface is rapidly depleted by reaction with TNT. The subsequent kinetics are rate limited by the formation of new reducing sites resulting in slower disappearance of TNT and less TAT formation. At high [Fe(0)], the initial supply of reducing sites exceeds the demand, resulting in faster disappearance of TNT and complete conversion to TAT.

In addition to the effect of [Fe(0)] described above, we have also found that the length of exposure of Fe(0) to water before adding the TNT also affects the appearance of products in solution. Longer "pre-exposure" times generate more products in solution, and better mass balances. Figure 6 illustrates this trend for 0, 1, and 2 days of pre-exposure. Additional data for other amounts of Fe(0) (not shown) support these results.

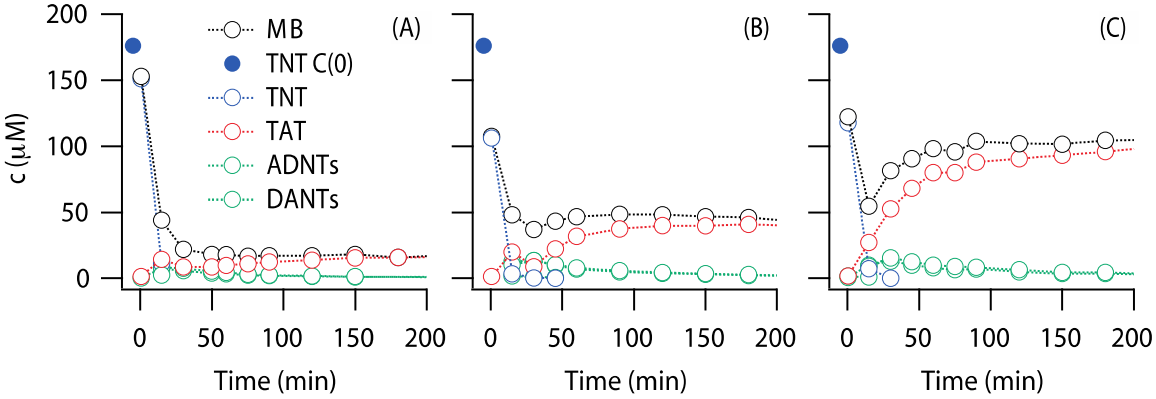

Figure 6. Effect of the length of pre-exposure time on TNT, products, and mass balance in batch experiments: (A) 0 days pre-exposure to solution, (B) 1 day, and (C) 2 days. In all cases, amount of Fe(0) = 3 g, and $[\text{TNT}]_0$ = 176 μM (shown as solid blue points). Some additional details regarding these results are described in (Miehr et al., 2003b) and a complete analysis will be published as (Miehr et al., 2003a).

The effect of "pre-exposure" time may be due to the same underlying processes as the effect of [Fe(0)] discussed above. One possibility is that both effects are due to greater reduction of the passive film with more time and/or capacity to generate reducing conditions. We tested this hypothesis, and several alternatives, with additional experimentation and modeling. This become a major theme in (Miehr et al., 2003a) because it has implications for the reactivity of Fe(0) with many other contaminants, including chlorinated solvents.

Respike Results (Tasks 1-2)[6]

Much of our laboratory work, as exemplified by the results in Figure 4 and Figure 6, has been done as single-spike batch experiments. However, batch experiments with serial respiking of reactants may be used to examine changes in the system as it approaches the steady-state conditions that apply to long-term column or field operation. In particular, we are interested in using respike experiments to examine the effect of passivation on the reactivity of the Fe(0). Ultimately, we hope that these respike experiments will help provide some general insights into how the controlling transformation processes scale from batch, column, and field.

Figure 7 shows the disappearance of TNT over multiple respikes with two respike intervals. The initial kinetics are well described by fitting a first-order disappearance model, as shown by the solid lines in the figure. The slope of these lines (i.e., k_{obs}) decreases with each respike. In Figure 7, the effect is more apparent for the shorter respike interval only because the time-scale is expanded.

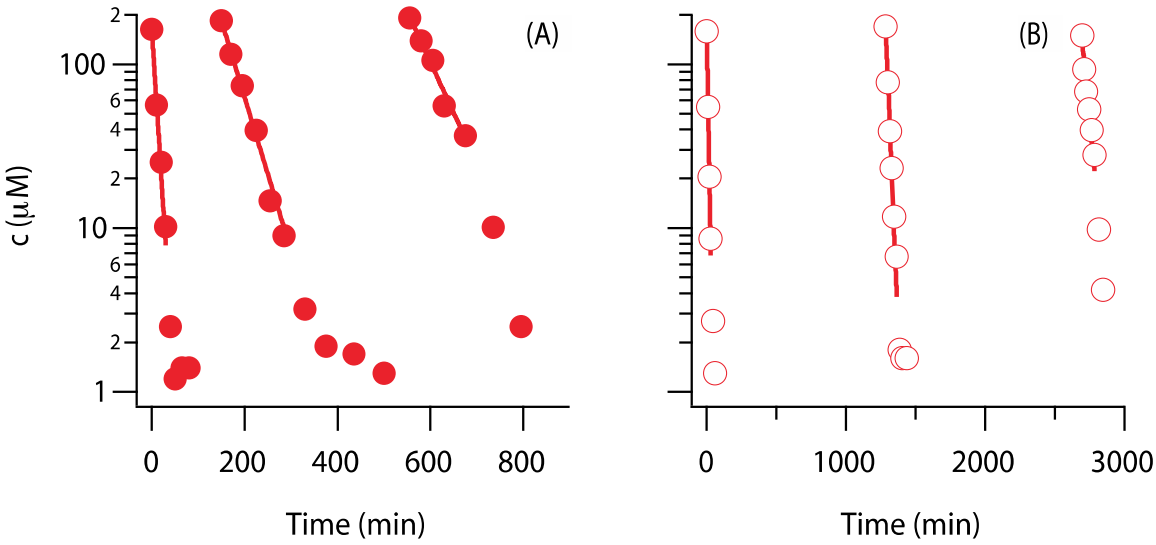

Figure 7. Effect of respike interval on batch experiments with TNT: (A) immediate respike (B) next day respike. Conditions: 4 g Peerless Fe(0) per 120 mL with 2 days of pre-exposure of Fe(0) to water prior to first addition of TNT.

To probe these effects further, we are investigating a range of experimental variables (such as respike concentration, time between respikes, or mass of iron). Figure 8 shows values of k_{obs} (from Figure 7 and additional experiments) plotted against the respike time and the respike number. The rate constants show a more consistent dependence on respike number than on respike time, suggesting that the passivation process is reaction driven, not spontaneous.

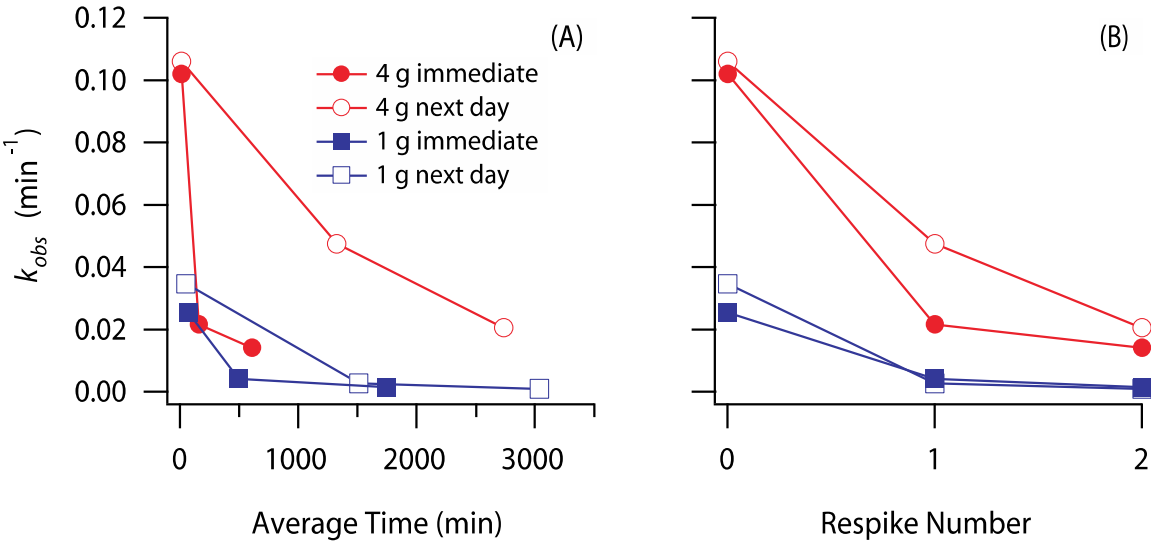

Figure 8. First-order rate constants, k_{obs}, for each respike experiment versus: (A) the average time for the corresponding respike data and (B) the number of the respike. Results are from batch experiments with 4 g and 1 g of Peerless Fe(0).

One possible mechanism for reaction driven-passivation is inhibition due to sorbed TNT reduction products. To model this, we assume that a fraction of the TNT degrades into some product that partitions to the Fe(0) surface blocking active sites. Prior evidence for this assumption can be found in (Devlin et al., 1998; Klausen et al., 2001; Oh et al., 2002b). Figure 9 shows the results of a simulated respike experiment with product inhibition compared to the experimental data from Figure 7. These results indicate that the product inhibition passivation mechanism is consistent with the observed passivation trends.

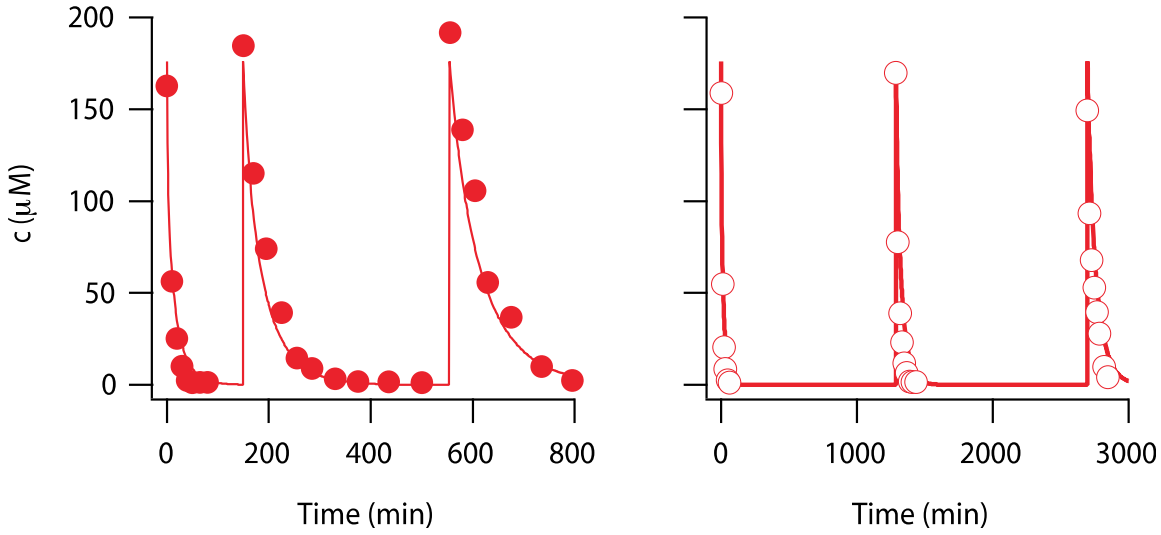

Figure 9. Simulations of the effect of product inhibition on respike experiments: (A) immediate respike (B) next-day respike. The simulations assume that accumulation of TNT reduction products on the iron surface decreases the reactivity of the iron.

Column Studies (Task 3)

Two sizes of columns have been used in this work. The larger columns are 2 cm i.d. x 15 cm long and the smaller columns are 1 cm i.d. x 5 cm long. We began with the larger columns, and found that they converted all TNT to TAT leaving no intermediate reduction products in the column effluent and apparently leaving little of the TNT residues bound to the solids in the column. This result is consistent with the trend we observed with increasing [Fe(0)] in batch experiments (i.e., more [Fe(0)] yields more TAT and better mass balances).

Figure 10 shows that this condition can be sustained for considerable time in the large columns. Even at high flow rates over many pore volumes, our large columns never gave breakthrough of TNT or any partial reduction products of TNT. Only TAT was observed in the column effluent, and the amount of TAT in the effluent matched the amount of TNT in the influent. Similar results have been obtained with laboratory column using groundwater from the Umatilla Weapons Depot (see below).

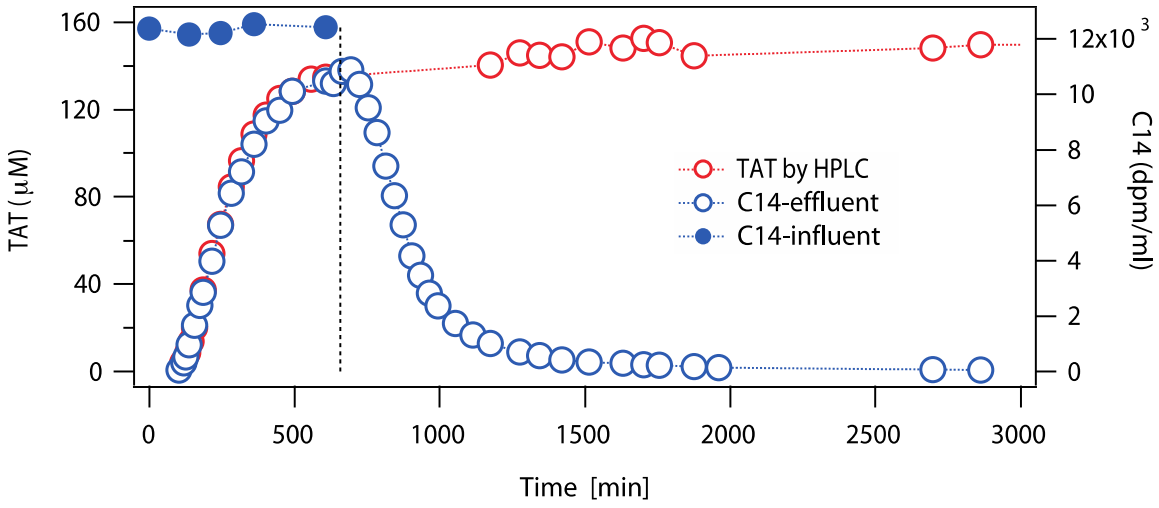

Figure 10. Breakthrough curves for total ^{14}C (by liquid scintillation counting on effluent fractions) and TAT concentration (by HPLC). Column was 2 x 15 cm, containing 180 g Peerless Fe(0), run at 1 mL min^{-1}, resulting in ca. 40 min/pore volume. Cold $[TNT]_0$ = 132 μM.

To investigate the breakthrough of TNT and its reduction products, we used a small column and high flow rate, which resulted in a contact time of only about 2 minutes. Figure 11 shows that breakthrough occurred under these conditions after ca. 500 pore volumes. Note that the order of breakthrough (DANTs first, then ADNTs, and TNT last) is the reverse of the order in which the species were introduced into (or formed within) the column. This suggests that the column results are influenced by processes in addition to simple (sorptive) retardation.

We hypothesized that the order of breakthrough shown in Figure 11 was due to gradually declining rates of reduction caused by passivation of the iron coupled with reduction of the TNT. Incorporating these effects into a reactive transport model allows us to simulate the observed effect.

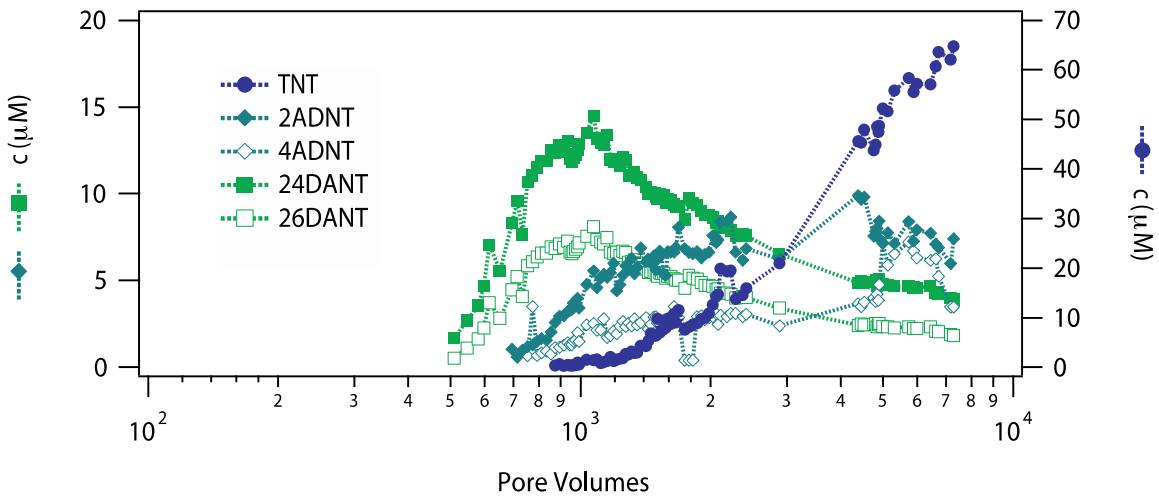

Figure 11. Partial breakthrough of TNT and intermediates on a small column (retention time ca. 2 minutes). Column was 1 x 5 cm, containing 18 g Peerless Fe(0), run at 1 mL min^{-1}, resulting in ca. 2 min/pore volume. $[TNT]_0$ = 132 μM.

Figure 12A shows breakthrough from a small column simulated using the model. This interpretation implies that there is a passivation front that propagates through the column with time. Figure 12B shows progress of the passivation front, as simulated by the model.

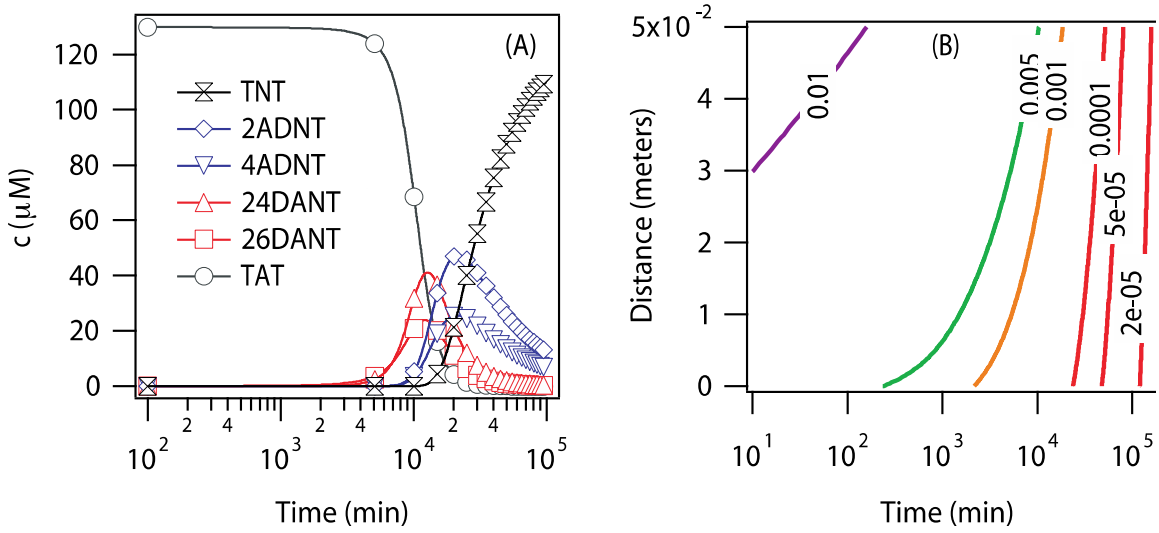

Figure 12. Simulation of reaction-driven iron passivation for TNT reacting in a column. Graphs show (A) simulated column effluent as a function of time, and (B) contours of constant active site concentration.

Fate of the Products (Tasks 1-3)[7]

Although essentially all TNT elutes as TAT under column conditions (recall Figure 10), small amounts may be retained on the Fe(0) as bound residue. Figure 13A shows that this less than 5%. Figure 13B shows that most of the bound-residue is located near the influent-end of the column. Figure 13C shows that only about 15% of the bound residue is extractable using the extractants we tested. Although the chemical state of this bound residue was difficult to determine, it is likely to include condensation products of the aromatic amines that result from reduction of the nitro groups of TNT.

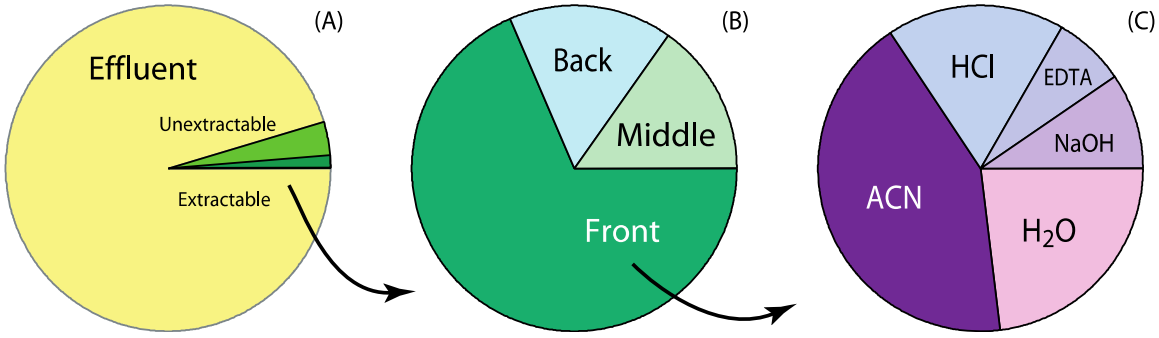

Figure 13. Percent recovery of ^{14}C-labelled residues by serial extraction of Fe(0) from a 15 cm column after 7 days exposure to 132 μM TNT. (A) Pie represents all ^{14}C added to the system, (B) pie represents spatial distribution of the (total) extractable residues, and (C) pie represents distribution among extracts performed serially on Fe(0) from the column front.

Since TAT is the major product of TNT reduction by Fe(0) under column (and presumably field) conditions, we used Fe(0) to generate TAT and studying the fate of this TAT under a range of conditions. Figure 14 shows that the stability of TAT in aqueous solution varies greatly with pH, and to a lesser degree with oxygenation. Loss of TAT at low pH appears to be due mainly to hydrolysis, but at high pH the dominant process appears to be auto-oxidation.

[7] Tratnyek, P. G.; R; Johnson, R. J. (in prep.) Environmental fate of 2,4,6-triaminotolune (TAT) and related reduction products of 2,4,6-trinitrotoluene (TNT).

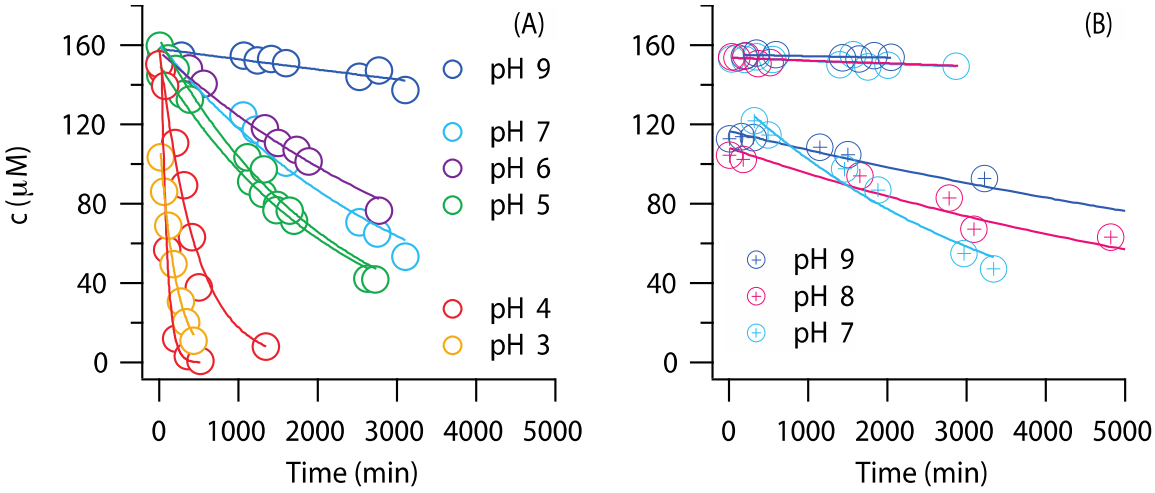

Figure 14. Disappearance of TAT in homogeneous batch systems: (A) effect of pH at 15 ºC, and (B) putative effects of oxygen at 22-27 ºC. These experiments done using TAT generated from an Fe(0) column, a range of buffers, and several temperatures. Incubations in the dark without mixing.

Most of the batch data for disappearance of TAT (e.g. those shown in Figure 14) fit simple, pseudo first-order kinetics. The resulting pseudo first-order rate constants (k_{obs}) vary systematically with pH, as shown in Figure 15. If the observed kinetics were controlled entirely by hydrolysis of TAT, we would expect them to fit the standard kinetic model for neutral and acid-catalyzed hydrolysis. The data in Figure 15 are qualitatively consistent with this model (black line is the model fit), but quantitative interpretation of this result is still in progress.

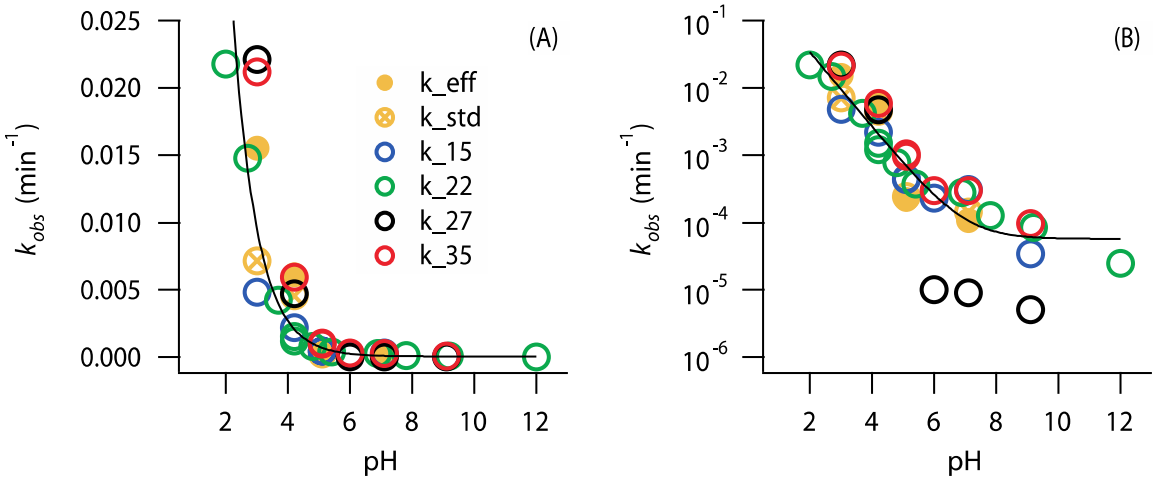

Figure 15. Effect of pseudo first-order rate constants on the disappearance of TAT: (A) linear plot, (B) log plot. At pH < 6 the relationship appears to be log-linear, but at pH > 6 the rate constants appear to be independent of pH.

Pilot-Scale Field Studies and Supporting Laboratory Column Studies (Task 4)[8]

Field Column Studies

To evaluate the performance of Fe(0) for removing TNT and RDX from groundwater from an actual contamination site, a series of pilot-scale column studies were evaluated at a pump-and-treat (P&T) operation at the Umatilla Chemical Storage Depot near Hermiston, OR. The P&T system extracts groundwater contaminated with TNT and RDX due to historical munitions manufacturing, and treats the effluent with granular activated carbon (U.S. Environmental Protection Agency, 2002). Figure 16 shows the experimental setup for the columns. A portion of the water coming into the plant was diverted to an automated mass flow control system, which maintained flows of 5 mL/min in up to three parallel columns. Each of the electropolished stainless steel columns was 15-cm long with an inside diameter (I.D.) of 2.45 cm. The columns were used to examine a range of possible ZVI/sand mixtures, from 10% by volume Peerless ZVI ("PMP Traditional", Size 8/50, from Peerless Powders and Abrasives, Detroit, MI) in 35/50 mesh silica sand to 100% ZVI of several grain sizes (Table 3). The approximate particle density of the Peerless iron was 7.5 g/cm^3 and the approximate porosity and bulk density of the iron were 0.55 and 3.4 g/cm^3, respectively.

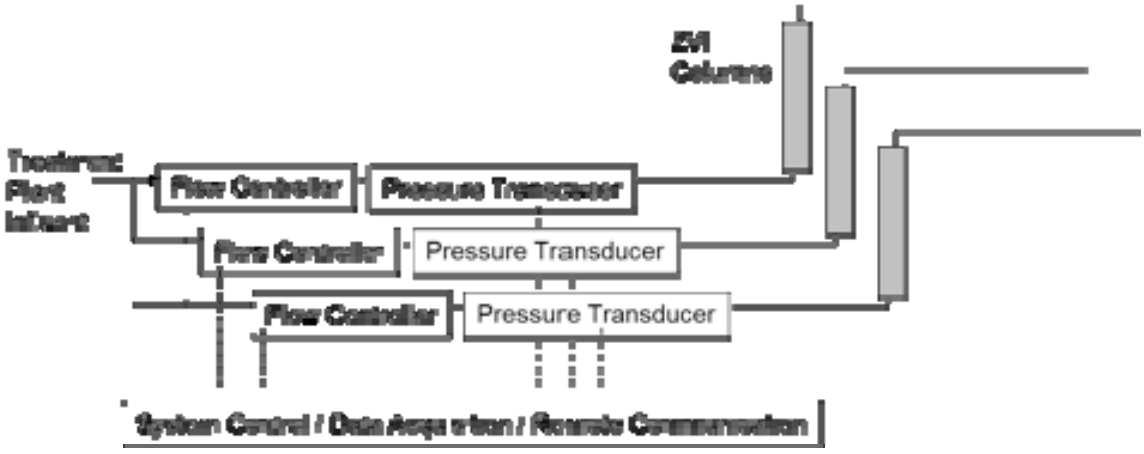

Figure 16. Schematic drawing of the column control system and columns used at the Umatilla site.

[8] Johnson, R. L.; Tratnyek, P. G.; Miehr, R.; Thoms, B. B.; Bandstra, J. Z. Reduction of hydraulic conductivity and reactivity in zero-valent iron columns by oxygen and TNT. *Ground Wat. Monitor. Remed.* **2005**, *25*, 129-136.

Table 3. Composition of the ZVI columns used at the Umatilla Chemical Storage Depot.

Column #	Percent ZVI by volume	ZVI mesh size	Percent sand By volume	Sand mesh size
1	10	35/50	90	35/50
2	20	35/50	80	35/50
3	30	35/50	70	35/50
4	100	35/50	0	-
5	100	18/35	0	-
6	100	8/18	0	-

Iron particle density and bulk density are ~7.5 g/cm^3 and ~3.4 g/cm^3, respectively.

Because of the remote location, the flow control system was designed to be accessible and controllable via cellular modem using an on-site laptop computer and remote control software. The pressure drop across each column was continuously monitored with pressure transducers and the data were logged to the laptop. Influent and effluent samples from the columns were collected on approximately a weekly basis to monitor degradation of the explosives by the columns.

Samples of the influent and effluent waters from the columns were collected by drawing 1 L of water through a Waters RDX SepPak at the column flow rate of 5 mL/min. The SepPak samples were subsequently processed by centrifugation to remove as much water as possible and then elution with 3 mL of acetone. 2,3-dinitrotoluene and 3,4-dinitrotoluene were used as internal standards, and analyses were performed on an HP5971A GC-MS using a DB-1MS column and selected ion monitoring. The detection limits were 0.01 μg/L for TNT and 0.1 μg/L for RDX, and influent concentrations were typically 5 μg/L for TNT and 50 μg/L for RDX. Breakthrough was recorded when effluent concentrations increased to 10 times the corresponding detection limits.

Experimental results from the six columns tested at the Umatilla field site are summarized in Figure 17. The cumulative flow through the columns is represented both in terms of pore volumes and as normalized volume. (The latter is defined as the cumulative volumetric flow through the column divided by the cross-sectional area of the column). Flow through the columns was terminated when pressure drop across the column reached 15-20 psi (initial pressure drop was on the order of 0.04 psi).

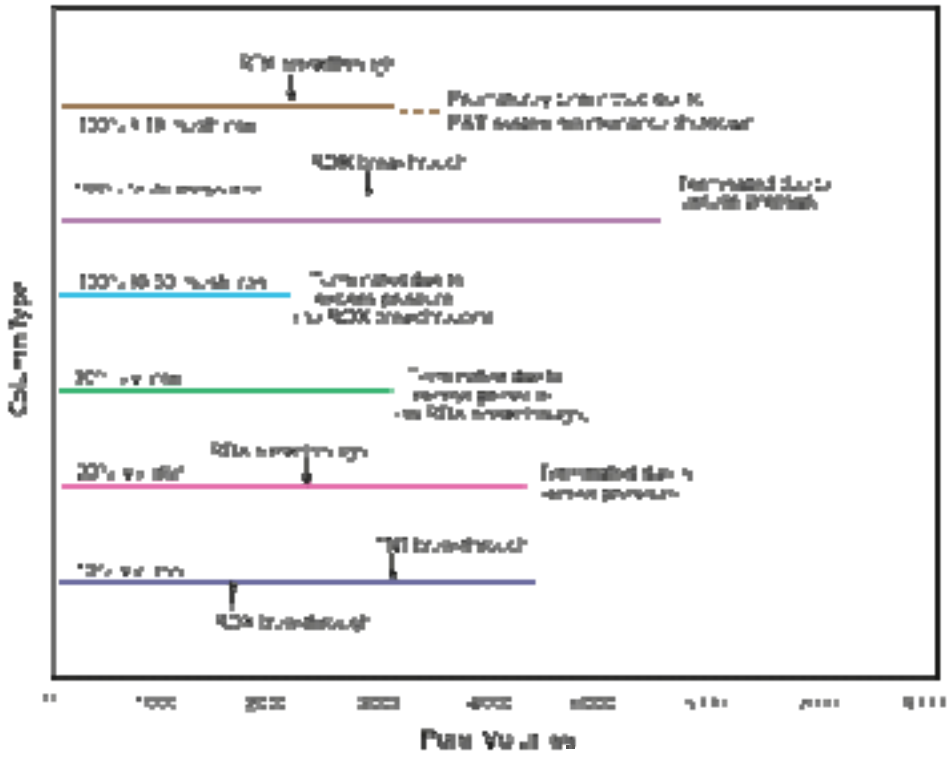

Figure 17. Summary of results for pilot-columns run at the Umatilla Chemical Storage Depot using groundwater diverted from an existing pump-and-treat system. All columns are 15 cm long by 2.5 cm in diameter. Flow rate is 5 mL min^{-1}. Porosity ranges from ~50% for 100% Fe(0) to ~38% for 10% Fe(0) v/v in silica sand. Residence times are 7.5 to 5.6 minutes, respectively.

With regard hydraulic conductivity loss, two trends are apparent from the data in Figure 17. First, the time to column plugging decreased with increasing iron content. Second, the time to column plugging increased with increasing iron grain size. In all cases, oxygen breakthrough was negligible throughout the duration of the experiments. Two conclusions can also be drawn from these data with regard to reactivity loss. First, the TNT and RDX breakthrough times increase with increasing iron content. Second, TNT and RDX breakthrough times decrease with increasing grain size. Thus, in the context of ex situ treatment of oxic groundwater, loss of reactivity may necessitate ZVI contents, which are too high to avoid significant K loss over time. The net effect in oxic cases is that it may be necessary to use a pre-column designed to remove oxygen followed by a higher-iron content column designed to remove explosives. As suggested by (Howson et al., 1996), this will allow a sufficiently high K to be maintained while providing a k_{sa} value large enough to ensure complete removal of the explosives.

Supporting Laboratory Column Studies

Laboratory column experiments were used as a compliment the field columns to examine the effects of oxygen and TNT on K and k_{sa} of the ZVI (Figure 18). Two identical columns were packed with 50% by volume 35/50 mesh Peerless iron in 35/50 mesh silica sand. Each column had an overall length of ~60 cm and an I.D. of 1.2 cm. Pressure/sampling points were located 0, 3, 10, 20, 30, 40, and 50 cm along the column. Each of the points was connected to a three-way valve, which was in turn connected to a Luer adaptor for sampling and a water manometer. 100% silica sand was used at the beginning and end of the columns and extended into the columns to the first and last sampling/pressure ports, respectively.

Prior to use, the columns were flushed with helium-sparged water to remove any trapped gas from the pore space. Following this, de-ionized water was delivered to the two columns after traveling through counter-current sparging towers to saturate one stream with air and the other with nitrogen. The water then flowed through ceramic-piston pumps, which controlled water flow to the columns at 1.0 mL/min. The columns were operated in an up-flow mode.

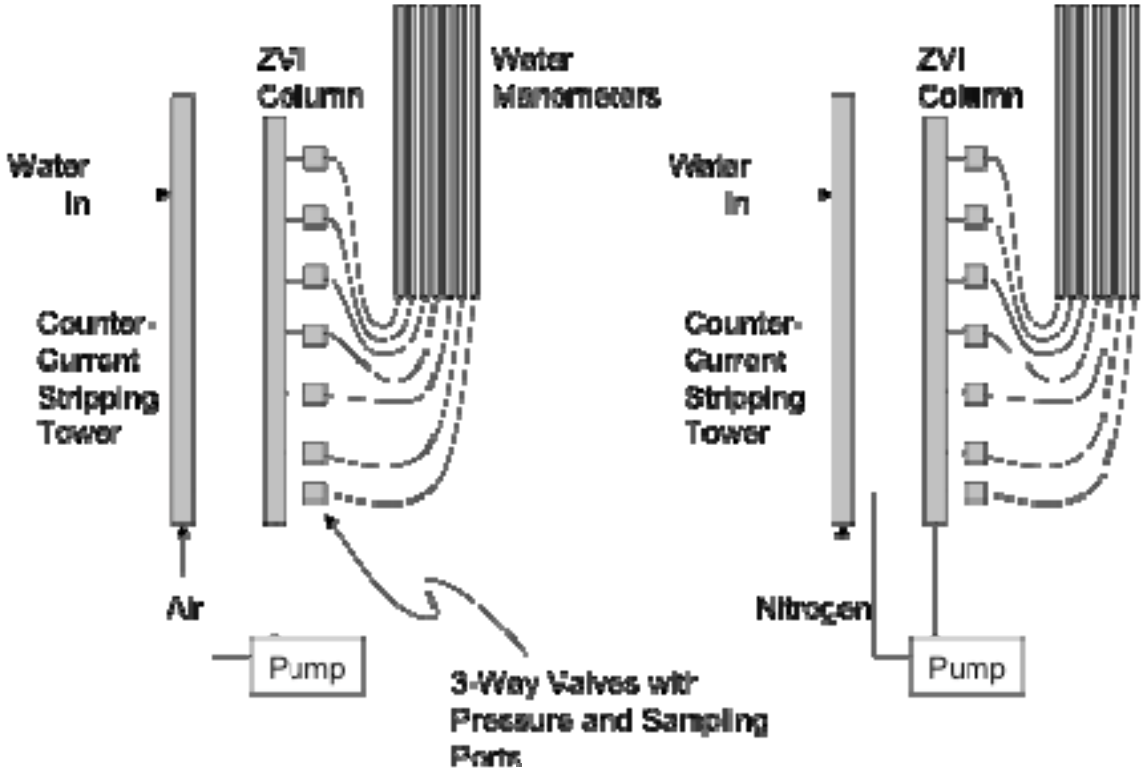

Figure 18. Schematic drawings of the laboratory columns.

The hydraulic conductivities of column intervals were determined using Darcy's law using the known flow rate and the distance and the observed pressure drop across each interval (i.e., between pressure ports). The water manometers allowed pressure drops between column ports of as small as 1 mm of water to be observed. Under normal flow conditions the pressure drop along the column was ~0.5 mm per centimeter, so hydraulic conductivity could be calculated from initial conditions through whatever changes occurred during the experiments. The pair of columns was operated for a period of ~28 days under these conditions and the pressure was recorded approximately daily.

On day 28, TNT was added to the feed water (10 mg/L). Because the sampling activities had a significant impact on pressure drop in the column, pressure measurements were discontinued during this phase of the experiment. Columns were operated with TNT for ~52 days with periodic sampling from all of the ports. The samples were analyzed for TNT by HPLC, using an Econosil C-18 column (length 250 mm, ID 4.6 mm; Alltech, Deerfield, IL). The mobile phase was 50:50 methanol/water at a flow rate of 1.1 mL min^{-1}. In all cases, TNT and degradation products were monitored with a UV detector at 254 nm.

On day 80, TNT was removed from the feed water and the columns continued to operate for another ~45 days in an unattended mode. At the end of that period the pressure drop at each point in the column was recorded. The columns were then frozen and cut into sections. The frozen sections were weighed, dried for 72 hours at 105^{o}C and re-weighed to determine water content. The water content was used to estimate porosity in the columns by assuming that the ratio of water content to the internal volume of each section was equal to the total porosity of that section at the conclusion of the experiment.

Figure 19 shows that during the first 28 days of operation (i.e., prior to TNT introduction) there was a two-order-of-magnitude reduction in *K* in the first three centimeters of the column. Almost as much reduction was observed in the 3-10 cm interval, with essentially no change in *K* in the remainder of the column. These data are consistent with those from (Mackenzie et al., 1999), who showed that, even after extended exposure, essentially all dissolved oxygen was consumed in the first 15 cm of their column. During the same period, *K* reduction in the oxygen-free column was negligible.

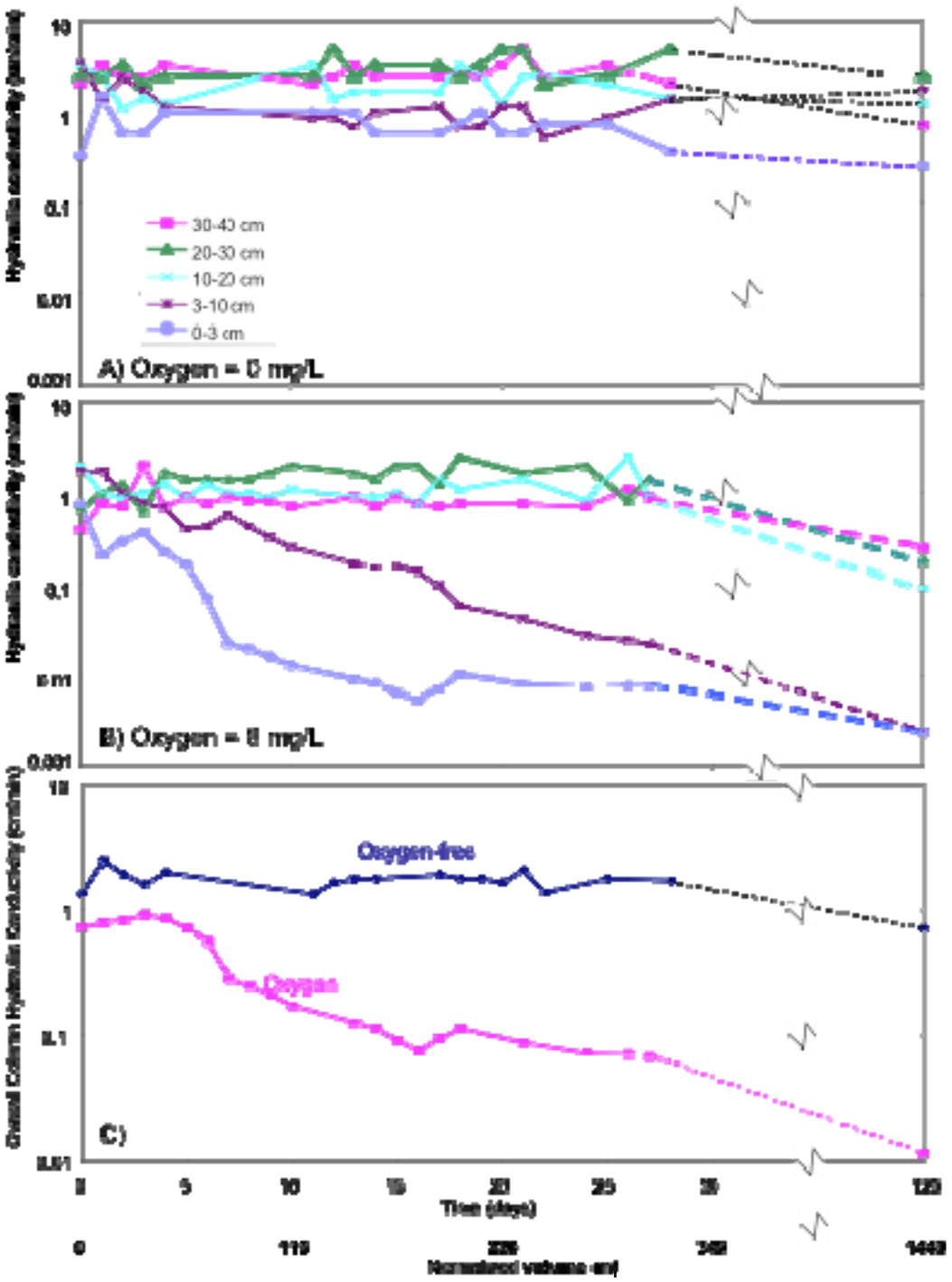

Figure 19. Hydraulic conductivity as a function of time for the individual sections of A) the oxygen free column; and B) the oxygen column. Overall hydraulic conductivity of the column as a function of time is shown in panel C).

When TNT (10 mg/L) was introduced into the columns, the oxygen-fed column showed a lower TNT reactivity in the first three centimeters of the column than the

oxygen-free column (Figure 20A). However, comparison of the two columns indicated that the overall effect of oxygen on TNT degradation was small. During the 52 days of operation with TNT, reactivity losses in the two columns were similar and substantial (Figure 20).

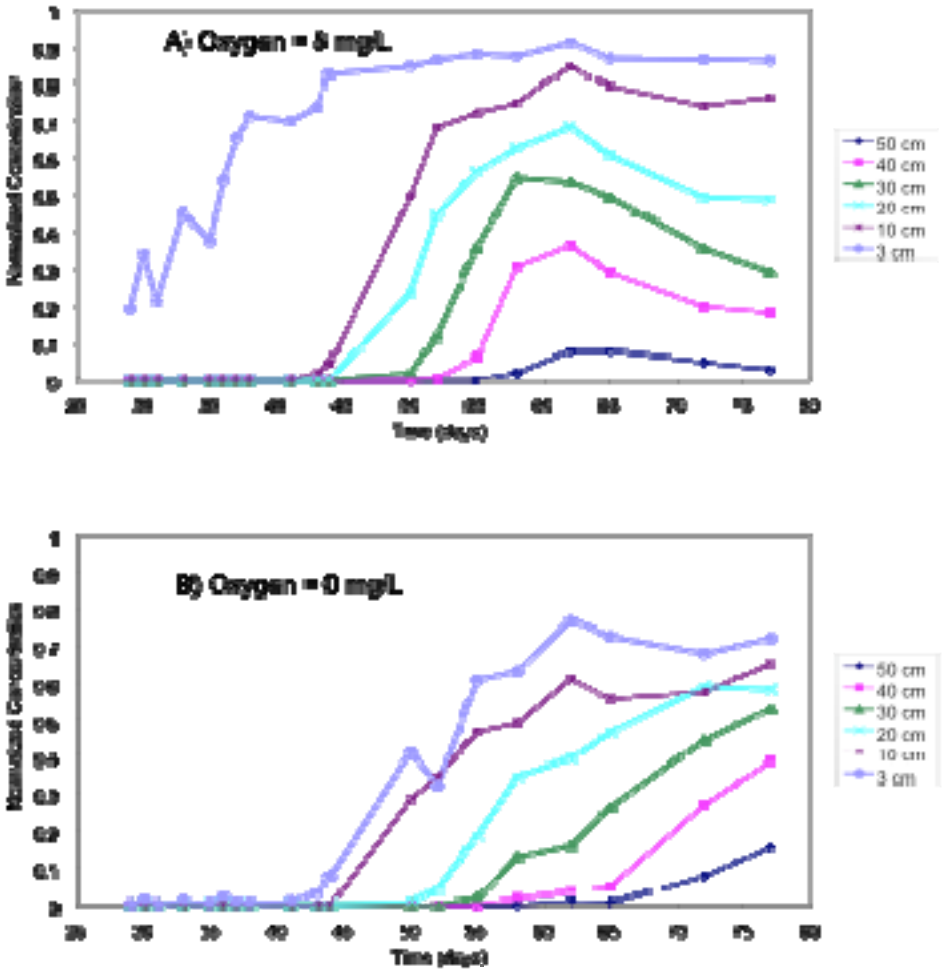

Figure 20. TNT breakthrough as a function of time at several distanced down the column for A) the oxygen column and B) the oxygen-free column.

Modeling Results (Task 5)

To aid in quantitative interpretation of the data in Figure 20, loss of reactivity in the columns was examined using three simple conceptual models. Pseudo-first order degradation of ZVI can be described as (Johnson et al., 1996):

$$\frac{d[P]}{dt} = -k_{SA} a_S \rho_m [P] \qquad [2]$$

where [P] is the reactant concentration (in this case TNT), k_{sa} is the surface-area normalized degradation rate constant, a_s is the specific surface area of the iron (m^2/g) and ρ_m is the mass concentration of iron (g /L of solution). However, degradation by ZVI depends not only on the physical surface area of the iron, but also on the density of active reaction sites on the surface of the iron. To represent this, Johnson et al. re-formulated eq. 2 as:

$$\frac{d[P]}{dt} = -k_2 \Gamma a_S \rho_m [P] \qquad [3]$$

where k_2 is the rate constant for reduction at the active sites and Γ is the surface concentration of active sites. In the context of active sites it is convenient to define the term [S_a] such that

$$[S_a] = \Gamma a_S \rho_m \qquad [4]$$

where [S_a] has units of moles of active sites per L of solution. Thus, the rate expression for disappearance of TNT can be written as:

$$\frac{d[TNT]}{dt} = -k_2^{TNT} [S_a][TNT] \qquad [5]$$

Changes in reactivity due to processes such as surface aging, adsorption of inhibitory species, and mineral precipitation may be incorporated into eq. 5 by developing an expression for [S_a] as a function of time (Johnson et al., 1996). In the present case, expressions for [S_a] are based on the following general reaction scheme:

$$TNT + S_a \xrightarrow{k_{aa}} TAT + S_a \qquad [6a]$$

$$xTNT + S_a \xrightarrow{k_{ap}} xTAT + S_p \qquad [6b]$$

where S_p denotes sites that are unreactive toward TNT, k_{aa} is the rate constant for TNT reductions that do not cause passivation, x is a stoichiometric factor which falls directly out of the three distinct passivation models described below, and k_{ap} is the rate constant for the passivation reaction, the precise interpretation of which depends on the value of x.

Model 1 assumes first-order reaction driven passivation. In this case the number of active sites [S_a] decreases linearly with the amount of TNT reduced. For this case the stoichiometric factor, x, equals one, and the rate law for [S_a] can be written as:

$$\frac{d[S_a]}{dt} = -\lambda k_2^{TNT} [S_a][TNT] \qquad [7]$$

where:

$$\lambda = \frac{k_{ap}}{k_{aa} + k_{ap}} \quad [8]$$

and

$$k_2^{TNT} = k_{aa} + k_{ap} \quad [9]$$

Note that in this model a fraction, λ, of the TNT reductions cause passivation and that eq. 7 is linear in $[S_a]$, indicating first-order reaction-driven passivation.

Model 2 assumes that reactivity decreases exponentially in proportion to the amount of TNT reduced. In this case $x = 0.5$ in eq. 6b and the rate expression can be written as:

$$\frac{d[S_a]}{dt} = -\lambda k_2^{TNT} [S_a]^2 [TNT] \quad [10]$$

Model 3 assumes that the reactivity of the entire column decreases exponentially over time. This is equivalent to setting $x = 0$ in eq. 6b and results in the rate expression:

$$\frac{d[S_a]}{dt} = -\beta [S_a] \quad [11]$$

where β is a first-order rate constant.

As formulated, eq. 11 does not explicitly assume that loss of reactivity is related to initial TNT concentration. However, evidence from a similar system (i.e., nitrotoluene and ZVI (Klausen et al., 2001)) supports the hypothesis that passivation in our system is driven by the diffuse reaction of TNT reduction products with the active iron sites.

Figure 21 shows both data from the laboratory columns (A-B) and results of the three models plotted as a function of distance down the column at eight time periods following the introduction of TNT (C-E). The results in Figure 21C-E were produced using spreadsheet models where the ZVI column was "divided" into 60 one-centimeter blocks and the reaction was assumed to be uniform within the blocks. To generate the model simulations, a TNT input concentration of 10 mg/L was used. Figure 21E shows that only model 3, where passivation occurs uniformly over the entire length of the column, comes close to matching the experimental data. A reduction in observed first-order rate constant from the previously-estimated value of 4,800 d^{-1} to 48 d^{-1} over the 52 day simulation was necessary to produce Figure 21E.

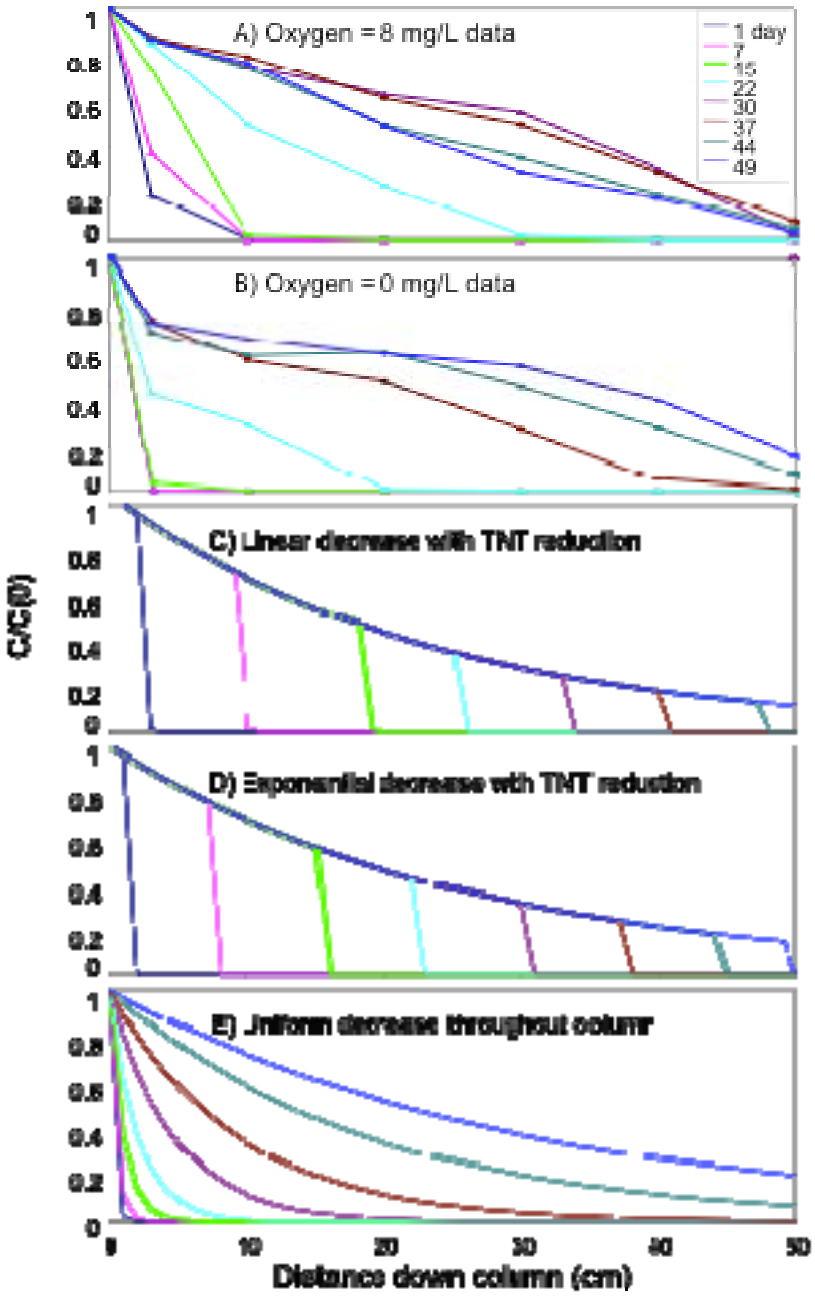

Figure 21. TNT concentration for the A) oxygen-fed and B) oxygen-free columns as a function of distance down the column at 1, 7, 15, 22, 30, 37, 44, and 49 days after introduction of TNT into the columns, and model simulations for the cases where: C) reactivity decreases linearly with TNT reduction; D) reactivity decreases exponentially with TNT reduction; and E) reactivity decreases uniformly over the entire length of the column

It is important to note that the models discussed below are conceptual and assume that passivation occurs as a first or second order process. Thus, while the data suggest

that uniform passivation of the columns, they do not provide a physical/chemical basis for that process.

At the end of the laboratory column experiment, the total porosity for the two laboratory columns was determined by water weight loss from column sections (Figure 22). The differences in porosity between the two columns were approximately the same as the experimentally-determined uncertainty in the measurements (±0.03). If it is assumed that porosity changes in the anoxic column were small, then the data indicate that there was little detectable porosity loss at the influent end of the oxic column. Based on a simple stoichiometric analysis, assuming either $Fe(OH)_2$ or Fe_3O_4 as products (with densities of 3.4 and 5.4 g cm^{-3}, respectively), during the first 15 days of column operation, the volume occupied by precipitates would have been between 0.10-0.16 cm^3. This corresponds to approximately one percent of the volume in the first 10 cm of the column. Over the full 125 days of column operation, approximately eight times as much precipitate would have been expected, and this quantity should have been detectable. However, as evidenced during the sampling phase, the precipitates were easily mobilized (i.e., they were not well attached to the porous medium), and as a result we anticipate that a significant fraction of the precipitate may have been able to exit the column. In either case, the rapid loss of K at the beginning of the experiment indicates that relatively small volumes of precipitate from the iron-oxygen reaction can have a significant impact on flow in the column.

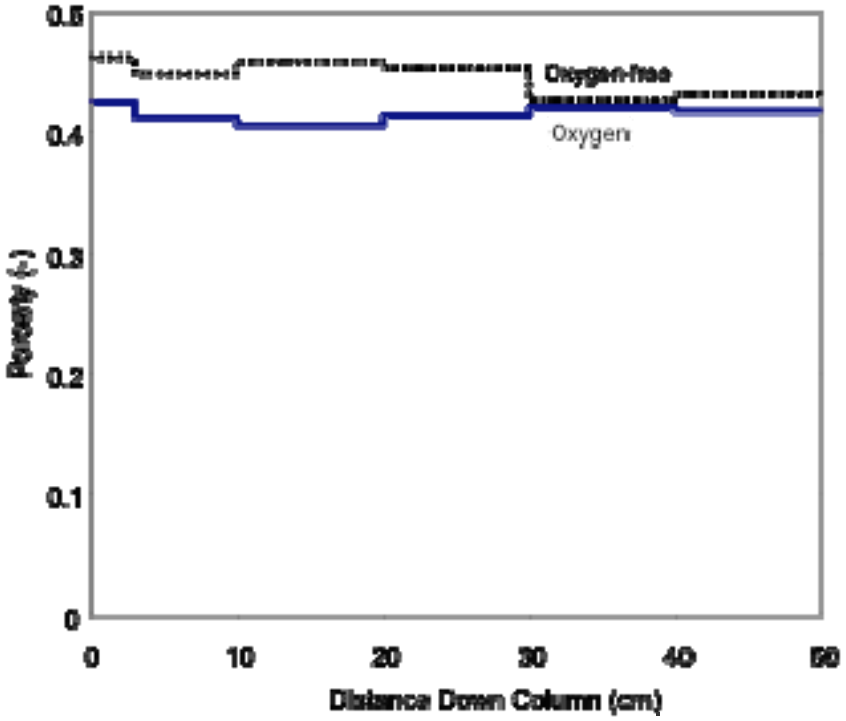

Figure 22. Total porosity as a function of distance down the column for the oxygen and oxygen-free columns.

Conclusions and Implications

Summary of Specific Conclusions

Iterating among batch and column experimental designs, combined with detailed diagnostic modeling, is providing a more detailed understanding of the processes controlling removal of TNT by Fe(0) than has been achieved with other contaminants to date. The iterative, multi-scale approach using Fe(0) as a model reductant, also provided new insights into the fate of TNT that may apply under other conditions. Specific results of general interest include:

- TNT is prone to give mixed-order disappearance kinetics due to site-saturation and other effects.
- Conversion of TNT to dissolved TAT approaches 100% with high concentrations of Fe(0) and longer time of exposure to solution (as in a column or PRB in the field).
- Respike data demonstrates reaction driven passivation of the iron due accumulation of adsorbed products of TNT reduction (presumably aromatic amines).

- Reaction driven passivation is also evident in column breakthrough data, where the most reduced species elute first and the parent compound, TNT, elutes last.
- TAT is fairly stable under anaerobic, high-pH conditions, but is rapidly transformed under the aerobic, low-moderate pH conditions.
- The field columns and supporting laboratory columns indicated that passivation of the ZVI over time was significant (e.g., a ~100X reduction over ~50 days), and passivation occurred over the full length of the column.
- The presence of dissolved oxygen in the influent water had a significant impact on the hydraulic conductivity of the ZVI, however its impact on reactivity of the ZVI was relatively small.

Implications for Future Research and Implementation

If the products of TNT reduction were retained on the Fe(0) surface, significant loss of reactivity (reaction-driven passivation) would be expected. However, it appears that under typical field conditions essentially all of the influent TNT will elute from the Fe(0)-bearing zone as TAT.

TAT appears to be fairly stable under conditions typical of an Fe(0)-bearing zone (i.e., no oxygen, high pH, and low natural organic matter). However, TAT is very labile to a number of transformations (hydrolysis, autoxidation, coupling) under typical aquifer conditions down-gradient from the Fe(0)-bearing zone (i.e., moderate pH, dissolved oxygen, and natural organic matter).

Therefore, we expect that an in situ Fe(0) permeable reactive barrier will fully reduce all aromatic nitro compounds, that most of these products will pass into the down-gradient aquifer, and that these products will be readily removed by "natural attenuation" in the down-gradient aquifer.

References

Agrawal, A., Ferguson, W.J., Gardner, B.O., Christ, J.A., Bandstra, J.Z. and Tratnyek, P.G., 2002. Effects of carbonate species on the kinetics of 1,1,1-trichloroethane by zero-valent iron. Environmental Science and Technology, 36(20): 4326-4333.

Arienzo, M., 2000. Use of abiotic oxidative-reductive technologies for remediation of munition contaminated soil in a bioslurry reactor. Chemosphere, 40(4): 441-448.

Bandstra, J.Z. and Tratnyek, P.G., 2003. Effects of surface heterogeniety on the kinetics of interfacial electron transfer, 225th National Meeting, 23-27 March 2002. Preprint Extended Abstracts, Division of Environmental Chemistry. American Chemical Society, New Orleans, LA, pp. in press.

Devlin, J.F., Klausen, J. and Schwarzenbach, R.P., 1998. Kinetics of nitroaromatic reduction on granular iron in recirculating batch experiments. Environmental Science & Technology, 32(13): 1941-1947.

Howson, P.E., Mackenzie, P.D. and Horney, D.P., 1996. Enhanced reactive metal wall for dehalogenation of hydrocarbons. Tertiary Enhanced reactive metal wall for dehalogenation of hydrocarbons, United States.

Hundal, L.S., Singh, J., Bier, E.L., Shea, P.J., Comfort, S.D. and Power, W.L., 1997. Removal of TNT and RDX from water and soil using iron metal. Environ. Pollut., 97(1/2): 55-64.

Johnson, T.L., Fish, W., Gorby, Y.A. and Tratnyek, P.G., 1998. Degradation of carbon tetrachloride by iron metal: Complexation effects on the oxide surface. Journal of Contaminant Hydrology, 29(4): 377-396.

Johnson, T.L., Scherer, M.M. and Tratnyek, P.G., 1996. Kinetics of halogenated organic compound degradation by iron metal. Environmental Science & Technology, 30(8): 2634-2640.

Klausen, J., Ranke, J. and Schwarzenbach, R.P., 2001. Influence of solution composition and column aging on the reduction of nitroaromatic compounds by zero-valent iron. Chemosphere, 44: 511-517.

Mackenzie, P.D., Horney, D.P. and Sivavec, T.M., 1999. Mineral precipitation and porosity losses in granular iron columns. J. Hazard. Mater., 68(1-2): 1-17.

Miehr, R., Bandstra, J.Z., Johnson, R.L. and Tratnyek, P.G., 2003a. Remediation of 2,4,6-trinitrotoluene (TNT) by iron metal: kinetic controls on product distributions in batch and column experiments. in prep.

Miehr, R., Bandstra, J.Z., Po, R. and Tratnyek, P.G., 2003b. Remediation of 2,4,6-trinitrotoluene (TNT) by iron metal: kinetic controls on product distributions in batch and column experiments, 225th National Meeting, 23-27 March 2002. Preprint Extended Abstracts, Division of Environmental Chemistry. American Chemical Society, New Orleans, LA, pp. in press.

Nam, S. and Tratnyek, P.G., 2000. Reduction of azo dyes with zero-valent iron. Water Research, 34(6): 1837-1845.

Oh, S.-Y., Cha, D.K. and Chiu, P.C., 2002a. Regio-selective reduction of dinitrotoluene mediated by graphite in scrap iron, 224th ACS National Meeting. Preprint Extended Abstracts, Division of Environmental Chemistry. Division of Environmental Chemistry, American Chemical Society, Boston, MA, pp. 542-544.

Oh, S.Y., Cha, D.K., Kim, B.J. and Chiu, P., 2002b. Effect of adsorption to elemental iron on the transformation of 2,4,6-trinitrotoluene and hexahydro-1,3,5-trinitro-1,3,5-triazine in solution. Environ. Toxicol. Chem., 21(7): 1384-1389.

Press, W.H., Flannery, B.P., Teukolsky, S.A. and Vetterling, W.T., 1988. Numerical Recipes in C. The Art of Scientific Computing. Cambridge University, Cambridge, England, 735 pp.

Scherer, M.M., Balko, B.A. and Tratnyek, P.G., 1998. The role of oxides in reduction reactions at the metal-water interface. In: D.L. Sparks and T.J. Grundl (Editors), Mineral-Water Interfacial Reactions: Kinetics and Mechanisms. ACS Symposium Series No. 715. American Chemical Society, Washington, DC, pp. 301-322.

Scherer, M.M., Johnson, K., Westall, J.C. and Tratnyek, P.G., 2001. Mass transport effects on the kinetics of nitrobenzene reduction by iron metal. Environmental Science and Technology, 35(13): 2804-2811.

Tratnyek, P.G., Miehr, R. and Bandstra, J.Z., 2002. Kinetics of reduction of TNT by iron metal, Groundwater Quality 2001: Third International Conference on Groundwater Quality. IAHS Red Book. IAHS Press, Sheffield, UK, pp. 427-433.

U.S. Environmental Protection Agency, 2002. Dynamic field activity study: Treatment system optimization, Umatilla Chemical Depot. EPA/540/R-02/007, Washington, DC.

Wüst, W.F., Köber, R., Schlicker, O. and Dahmke, A., 1999. Combined zero- and first-order kinetic model of the degradation of TCE and cis-DCE with commercial iron. Environ. Sci. Technol., 33(23): 4304-4309.

Appendices

Journal Articles

1. Tratnyek, P. G.; Miehr, R.; Bandstra, J. Z. (**2002**) Kinetics of reduction of TNT by iron metal; *Groundwater Quality 2001: Third International Conference on Groundwater Quality,* Sheffield, UK, IAHS Press, Vol. No. 275, pp. 427-433.
2. Bandstra, J. Z.; Tratnyek, P. G. Applicability of single-site rate equations for reactions on inhomogenous surfaces. *Indus. Eng. Chem. Res.* **2004**, *43*, 1615-1622.
3. Miehr, R.; Tratnyek, P. G.; Bandstra, J. Z.; Scherer, M. M.; Alowitz, M. J.; Bylaska, E. J. Diversity of Contaminant Reduction Reactions by Zerovalent Iron: Role of the Reductate. *Environ. Sci. Technol.* **2004**, *38*, 139-147.
4. Bandstra, J. Z.; Miehr, R.; Johnson, R. L.; Tratnyek, P. G. Reduction of 2,4,6-trinitrotoluene (TNT) by iron metal: kinetic controls on product distributions in batch experiments. *Environ. Sci. Technol.* **2005**, *39*, 230-238.
5. Johnson, R. L.; Tratnyek, P. G.; Miehr, R.; Thoms, B. B.; Bandstra, J. Z. Reduction of hydraulic conductivity and reactivity in zero-valent iron columns by oxygen and TNT. *Ground Wat. Monitor. Remed.* **2005**, *25*, 129-136.
6. Miehr, R; Johnson, R. J.; Tratnyek, P. G. (in prep.) Environmental fate of 2,4,6-triaminotolune (TAT) and related reduction products of 2,4,6-trinitrotoluene (TNT). *Environ. Sci. Technol*.

Proceedings Papers

7. Tratnyek, P. G.; Miehr, R.; Bandstra, J. Z. (2002) Kinetics of reduction of TNT by iron metal; *Groundwater Quality 2001: Third International Conference on Groundwater Quality,* Sheffield, UK, IAHS Press, Vol. No. 275, pp. 427-433.
8. Miehr, R.; Bandstra, J. Z.; Po, R.; Tratnyek, P. G. (2003) Remediation of 2,4,6-trinitrotoluene (TNT) by iron metal: Kinetic controls on product distributions in batch and column experiments; *225th National Meeting, 23-27 March 2002,* New Orleans, LA, American Chemical Society, Vol. 43, No. 1, 644-648.
9. Bandstra, J. Z.; Tratnyek, P. G. (2003) Effects of surface heterogeniety on the kinetics of interfacial electron transfer; *225th National Meeting, 23-27 March 2002,* New Orleans, LA, American Chemical Society, Vol. 43, No. 1, 541-545.

Theses

10. Bandstra, J. Z. Kinetic Modeling of Heterogeneous Chemical Reactions with Applications to the Reduction of Environmental Contaminants on Iron Metal. Ph.D. Thesis, Oregon Health & Science University, **2005**.